AGU PUBLICATIONS

Geophysical Research Letters

RESEARCH LETTER
10.1002/2014GL059608

Key Points:
- Submesoscales generate interannual variations in phytoplankton blooms
- The variability occurs at local scale and translates to larger scale
- High horizontal resolution is needed to fully capture it

Correspondence to:
M. Lévy,
marina.levy@upmc.fr

Citation:
Lévy, M., L. Resplandy, and M. Lengaigne (2014), Oceanic mesoscale turbulence drives large biogeochemical interannual variability at middle and high latitudes, *Geophys. Res. Lett.*, *41*, 2467–2474, doi:10.1002/2014GL059608.

Received 12 FEB 2014
Accepted 20 MAR 2014
Accepted article online 24 MAR 2014
Published online 7 APR 2014

Oceanic mesoscale turbulence drives large biogeochemical interannual variability at middle and high latitudes

Marina Lévy[1,2], Laure Resplandy[3], and Matthieu Lengaigne[1,2]

[1]Sorbonne Universités, UPMC Univ. Paris 06, CNRS, IRD, MNHN, UMR 7159 LOCEAN-IPSL, Paris, France, [2]Indo-French Cell for Water Sciences, IISc-NIO-IITM-IRD Joint International Laboratory, NIO, Goa, India, [3]SCRIPPS, La Jolla, California, USA

Abstract Observed phytoplankton interannual variability has been commonly related to atmospheric variables and climate indices. Here we showed that such relation is highly hampered by internal variability associated with oceanic mesoscale turbulence at middle and high latitudes. We used a 1/54° idealized biogeochemical model with a seasonally repeating atmospheric forcing such that there was no external source of interannual variability. At the scale of moorings, our experiment suggested that internal variability was responsible for interannual fluctuations of the subpolar phytoplankton bloom reaching 80% in amplitude and 2 weeks in timing. Over broader scales, the largest impact occurred in the subtropics with interannual variations of 20% in new production. The full strength of this variability could not be captured with the same model run at coarser resolution, suggesting that submesoscale resolving models are needed to fully disentangle the major drivers of biogeochemical variability at interannual time scales.

1. Introduction

Analyses of ocean color observations reveal significant interannual variations in net annual primary production [*Rousseaux and Gregg*, 2014] and in timing and amplitude of seasonal phytoplankton blooms [*Cole*, 2013]. Coherent patterns of this variability at the scale of ocean basin have been successfully attributed to climate indices [*Behrenfeld et al.*, 2006; *Chavez et al.*, 2011]. At the scale of time series stations or ocean color pixels, changes in local atmospheric conditions can also partly explain the observed changes [e.g., *Henson et al.*, 2006]. However, particularly at middle and high latitudes, the strength [*Follows and Dutkiewicz*, 2001] and timing [*Cole*, 2013] of phytoplankton blooms are not always connected with changes in meteorological forcing. This suggests that internal oceanic fluctuations might feed the observed interannual variability.

Natural candidates for middle and high latitudes' internally driven variability are mesoscale eddies and the complex web of submesoscale fronts associated with them, i.e., the "ocean weather" [*Williams et al.*, 2007]. Eddy-permitting ocean circulation models suggest that the intrinsic variability associated with this mesoscale turbulence might be responsible for interannual variability in physical properties such as eddy kinetic energy [*Penduff et al.*, 2004], mode water formation [*Hazeleger and Drijfhout*, 2000], sea level anomaly [*Penduff et al.*, 2011], and meridional overturning [*Thomas and Zhai*, 2013]. Moreover, a variety of recent observations and modeling experiments support the idea that mesoscale turbulence influences phytoplankton growth by affecting both the nutrient and light environments [*Lévy et al.*, 2012a, and references therein]. At subpolar latitudes, the increased rate of stratification at mesoscale [*Levy et al.*, 1998] or submesoscale [*Karleskind et al.*, 2011; *Mahadevan et al.*, 2012] fronts may advance the timing of the bloom. In the subtropics, episodic nutrient injections into the euphotic layer by eddies [*McGillicuddy et al.*, 1998] and submesoscale fronts [*Lévy et al.*, 2001] act to increase primary production. The net impact on an annual time scale will depend on how many fronts and eddies have been passing by. Through these mechanisms, the chaotic nature of mesoscale turbulence should induce interannual variations in phytoplankton phenology and net annual primary production.

In this study, we investigated the interannual variability in phytoplankton phenology driven by the intrinsic, chaotic high-frequency ocean variability associated with mesoscale turbulence. More specifically, we addressed the following questions: Does internal variability contribute to significant interannual variability in the timing and amplitude of seasonal, surface phytoplankton blooms at the local scale? What are the underlying processes? Does this contribution translate to biogeochemically relevant fluxes at larger scale? What model resolution is needed to capture it? To answer these questions, we used 5 years of an idealized, submesoscale permitting ocean biogeochemical primitive equation model experiment where year-to-year

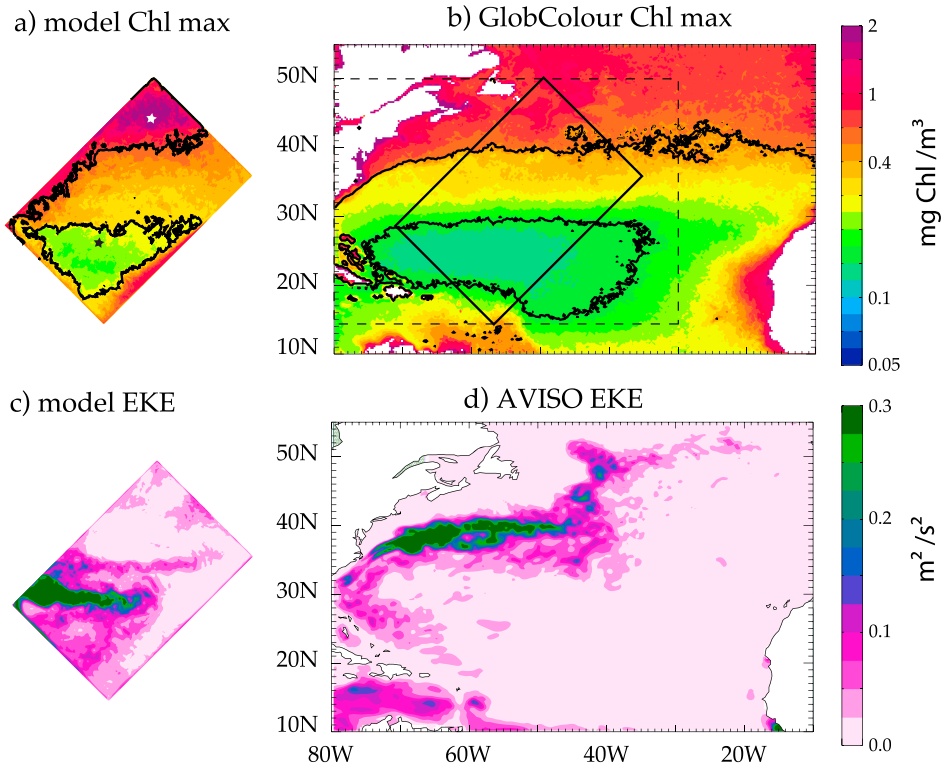

Figure 1. Comparison of chlorophyll peak and eddy kinetic energy (EKE) in the model and observed from space in the North Atlantic. (a) Median value of chlorophyll peak over the 5 years of model outputs. (b) Median value of chlorophyll peak over 15 years of satellite ocean color data (GlobColour product). (c) Annual mean eddy kinetic energy in the model. (d) Annual mean eddy kinetic energy computed from the AVISO satellite altimetry product. The black lines in Figures 1a and 1b mark the contours which were used to delimitate the boundaries of the subtropical and subpolar zones in Figure 3. The model rotated rectangle is reported in Figure 1b for illustration purpose only. The dashed rectangle in Figure 1b is the area over which data analyses shown in Figures 3a and 3b were performed. The white (respectively black) star in Figure 1a shows the position of the subpolar (respectively subtropical) virtual mooring used in Figure 2.

variations in the atmospheric forcing were excluded [*Lévy et al.*, 2012b]. We repeated the same experiment at progressively decreasing horizontal resolution until internally driven interannual variations eventually vanished. The model configuration mimicked the North Atlantic stratified subtropics and strongly seasonal subpolar regimes. This allowed us to compare the internally driven variability in the model to the observed variability in North Atlantic ocean color data at similar latitudes.

2. Method

We used an idealized configuration of the primitive equation model Nucleus for European Modelling of the Ocean (NEMO) [*Madec*, 2008] used in conjunction with the biogeochemical model LOBSTER (Lodyc Ocean Biogeochemical System for Ecosystem and Resources) [*Lévy et al.*, 2012b]. This configuration resolved features analogous to a Western boundary current, stratified subtropics, and strongly seasonal subpolar regimes at high resolution [*Lévy et al.*, 2012b]. A large number of interacting, transient mesoscale eddies were spontaneously and chaotically generated. We examined how this internal eddy variability induced year-to-year variations in key biogeochemical metrics.

The model domain was a rotated rectangle, bounded by vertical walls and by a flat bottom that covered the latitudinal range 15°N to 50°N (Figure 1). The circulation was forced by a repeating annual cycle of zonal wind and buoyancy fluxes, which varied seasonally in a sinusoidal manner between winter and summer extrema. Thus, there was no variability at intraseasonal or interannual time scales in the forcings. The horizontal resolution was submesoscale permitting (1/54°). The biogeochemical model LOBSTER solves for phytoplankton, zooplankton, detritus, dissolved organic matter, nitrate, and ammonium. The model was integrated for 55 years from an initial state derived after 1000 years of integration at low (1°) resolution from

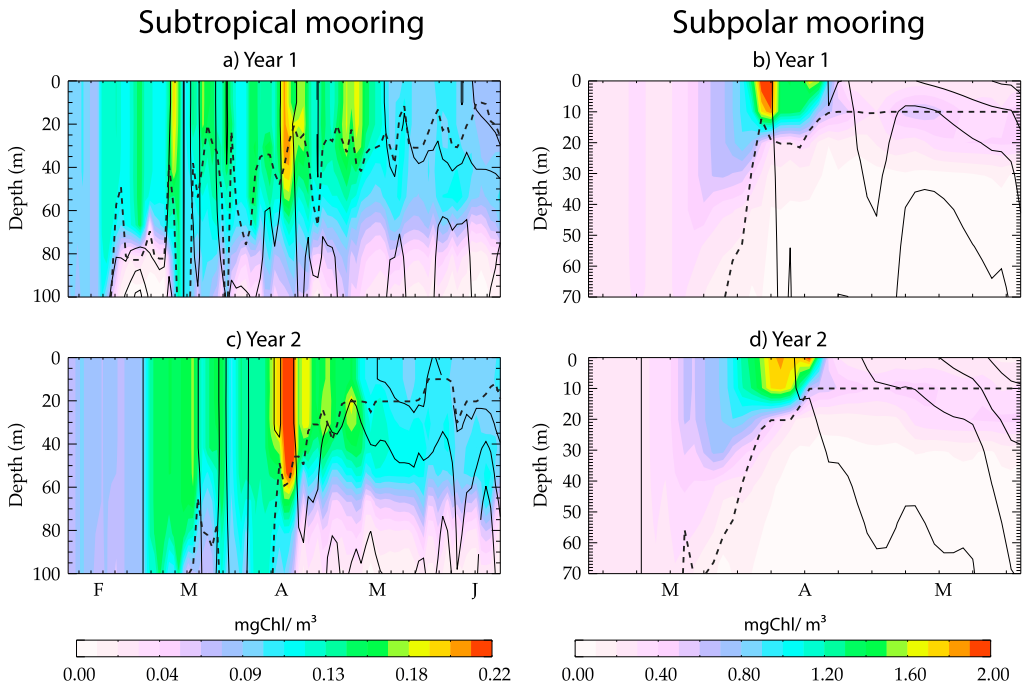

Figure 2. Illustration of phytoplankton variability over two consecutive years in the model, at the two virtual moorings, (a and c) subtropical and (b and d) subpolar, shown in Figure 1a. The thin black lines are isopycnals and the dashed line is the mixed-layer base. Note that different time periods are shown at the two moorings

constant density and nitrate profiles. An initial drift disappeared after ~30 years [see Figure 2 in *Lévy et al.*, 2012b]. Due to storage limitation, only the last 5 years were saved at high temporal resolution (every 2 days). Outputs were then coarsened on a 1/9° grid (corresponding to the effective model resolution [*Lévy et al.*, 2012c]). More detailed information about the model configuration, closures, and parameters can be found in *Lévy et al.* [2010, 2012b]. We focused on interannual variability of three metrics: the timing and the amplitude of the seasonally recurrent surface chlorophyll bloom peak, which can be easily assessed from ocean color observations; and the annual mean new production (defined as the net primary production supported by nitrate), which is more relevant from a biogeochemical perspective. Interannual variability was estimated by computing the standard deviation σ of the three metrics over the 5 years of simulation at each grid point. We defined the interannual variability range as 2σ, and we expressed it as a percentage of the mean value for peak amplitude and new production and in days for peak timing. The sensitivity of our results to the limited 5 year sampling will be addressed in section 4. Ranges showed coherent patterns over the subpolar and subtropical regions. Thus, for the sake of brevity, we arbitrarily delimited a subpolar and a subtropical zone using two contours of phytoplankton peak amplitude (Figure 1a) and discussed our results in terms of the median value of the range over each of these two zones. These median values were fairly insensitive to the choice of the contour values used to define the boundaries.

3. Results

The main features of the model solution [*Lévy et al.*, 2010, 2012b] are briefly reminded. The forcing generates a strong jet, which runs diagonally across the domain at ~30°N and separates a nutrient-depleted subtropical region south of 30°N from a nutrient-rich subpolar region north of 36°N, with a transition intergyre region in between. The jet is baroclinically unstable, and this instability is the main source of eddy energy in the model. The eddy kinetic energy (EKE) shows patterns and intensity comparable to those observed in the North Atlantic (Figures 1c and 1d). The model also captures the strong contrast in phytoplankton peak amplitude that is observed between the oligotrophic subtropical North Atlantic and the more productive subpolar North Atlantic (Figures 1a and 1b).

Phytoplankton profiles at two virtual moorings in the model subtropical and subpolar gyres (stars in Figure 1a) over 2 consecutive years serve to illustrate year-to-year variability of the model phenology

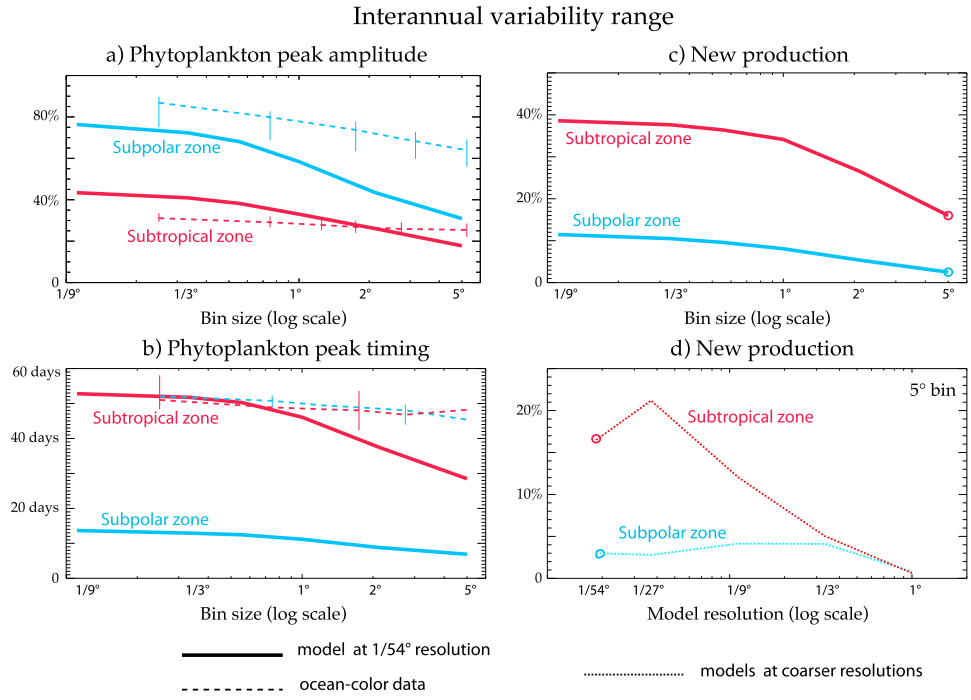

Figure 3. Interannual variability range against bin size for (a) phytoplankton peak amplitude, (b) phytoplankton peak timing, and (c) annual mean new production. Shown are median values over the subtropical (red) and subpolar (blue) zones delimited in Figure 1. Thick lines show the range in the 1/54° resolution model simulation. Dashed lines show the range in ocean color data, with vertical bars indicating the 25%–75% quartile resulting from randomly undersampling 5 of the 15 available years. (d) Range in new production binned at 5° against model grid resolution. Open circles in Figures 3c and 3d both show the range in new production binned at 5° in the 1/54° resolution simulation.

(Figure 2). Given that the atmospheric forcing is climatological, if internal variability was negligible, we would expect the seasonal time evolution of phytoplankton to repeat itself identically. This was clearly not the case. Instead, at both moorings, the seasonal evolution was strongly disrupted by intraseasonal events. These events were associated with the chaotic passage of submesoscale density fronts (black contours in Figure 2).

The qualitative results at the two moorings were then generalized to the entire subtropical and subpolar zones. At the scale of model pixels (1/9° bins in Figures 3a and 3b), the model showed interannual variability in phytoplankton peak timing close to 2 months in the subtropical zone and 2 weeks in the subpolar zone. Ranges in phytoplankton peak amplitude were close to 80% in the subpolar zone and 40% in the subtropics. Variability in the intergyre zone located in between the subpolar and subtropical zones was somehow intermediate and is not shown here.

As illustrated in Figure 2, variability at this local scale was related to the passage of submesoscale fronts in this model. One might thus expect the variability to decrease after averaging over larger scales, as positive and negative anomalies associated to fronts might partially cancel out. In order to evaluate how much of the local variability was retained at larger scale, we binned the phytoplankton fields prior to computing ranges, with bin size 1/3°, 1/2°, 1°, 2°, and 5° (Figure 3). As expected, ranges started to significantly decrease as bin size increased above the eddy decorrelation length scale (>1°). Nevertheless, variability did not cancel out and on the contrary remained rather large for the largest 5° bins, with 1 (respectively 3) weeks for peak timing and 30% (respectively 20%) for peak amplitude in the subpolar (respectively subtropical) zone.

Perhaps most importantly, internal variability led to significant interannual variations of the model annual mean new production (Figure 3c), notably in the subtropical region, with variations ranging from 40% at the local scale (1/9° bins) to nearly 20% at the large scale (5° bins). In contrast, in the subpolar region, the variability in new production was not as marked (10% at 1/9° and less than 5% at 5°). This might be surprising given the relatively large variability in phytoplankton peak amplitude in the subpolar zone.

High horizontal resolution is a necessary condition to simulate intense mesoscale eddy fields and associated submesoscale fronts. The same model run at 1/9° horizontal resolution instead of 1/54° showed significantly lowered EKE, associated with fewer, shorter-lived, and less intense eddies [*Lévy et al.*, 2010]. In order to assess which model resolution is needed to capture the full strength of the internally driven interannual variability, we used a series of similar model experiments run at decreasing horizontal resolution (1/27°, 1/9°, 1/3°, and 1°, see *Lévy et al.* [2012c]). We found a sharp decrease in internally driven interannual variability of new production in the subtropical zone when the resolution was below submesoscale permitting (>1/27°, Figure 3d). The simulation with a resolution of 1/9° could only capture half of the interannual variability simulated at 1/54°, and this dropped to less than one third with a resolution of 1/3°. At 1° resolution, eddy variability was entirely suppressed and interannual variability vanished.

4. Discussion

Our model revealed significant interannual variability in surface phytoplankton bloom phenology, namely, in phytoplankton peak timing and peak amplitude. The simulated interannual variability ensued from subseasonal variations associated to the passage of submesoscale fronts. These fronts perturbed the mean seasonal cycle in a random manner, which lead to year-to-year fluctuations (Figure 2). These variations were large at the local scale of a model's pixel, and did not cancel out after 5° binning (Figure 3). This suggested that interannual variations in ocean color images binned over scales of 1° to 5°, as those commonly used for the study of large-scale bloom dynamics [*Martinez et al.*, 2009; *Behrenfeld*, 2010], arise not only from external processes (atmospheric/climate forcings) but also from internal processes associated with mesoscale turbulence. This might partly elucidate why climate indices, although useful indicators, can never fully explain the observed variability.

Interannual variability in our model resulted solely from internal processes, a contribution which is difficult to disentangle from observations alone. As a crude attempt to gain some insight on the relative importance of internal variability to total interannual variability, we have repeated the interannual variability range analysis using ocean color observations (dashed lines in Figures 3a and 3b). We used 15 years of multisatellite 8 days chlorophyll composites available at 1/4° resolution (Glocolour product, http://www.globcolour.info/). Due to the very idealized nature of our model configuration, comparing the variability in the model and in these observations is only indicative. Despite the limitation due to the idealized nature of our experiment, we found as expected that the interannual variability in the observations was larger than in the model over 5° bins. Next we stipulate, for the purpose of this discussion, that this extra amount of variability ensued from climate variability and atmospheric synoptic events. Interestingly, this rough comparison suggested that, both in the subpolar and subtropical zones, roughly half of the observed large-scale variability in phytoplankton peak amplitude might be attributable to internal variability. This was also the case regarding large-scale phytoplankton peak timing in the subtropics. In contrast, only ~1/5 of the observed variability in peak timing in the subpolar zone could be explained by internal variability, suggesting that the remaining 4/5 may be atmospherically driven. At small scale, the amplitude of small-scale interannual variability in the observations is likely to be underestimated, due to the large amount of missing data at this time and space scale [*Cole et al.*, 2012]. This underestimation, along with our model deficiencies, could explain some mismatches between the modeled and observed levels of variability for small bin size: the slopes of the phytoplankton peak timing and peak amplitude ranges against bin size were not as steep in the observations as they were in the model, particularly in the subpolar zone, and the observed levels of variability for phytoplankton peak amplitude in the subtropics were unexpectedly below model estimates.

However, as stated above, these estimations must be handled with great care due to the simplicity of our model. A more reliable assessment would require a realistic model configuration forced with the full spectrum of atmospheric variability. If this realistic model captured the same amount of variability than in the observations, it would be possible to isolate the contribution of internal drivers to interannual variability by performing a twin model experiment forced by a repeating seasonal cycle as in *Penduff et al.* [2011].

Moreover, in our model, mesoscale turbulence is the only source of internal variability. Evidence for this is that interannual variability cancels out when the model is run at 1° resolution (Figure 3d). However, internal variability in the ocean might also arise from other processes not well captured in our model, such as unforced interdecadal modes of the thermohaline circulation [*Huck et al.*, 2001] or oscillations in population dynamics [*Poggiale et al.*, 2013].

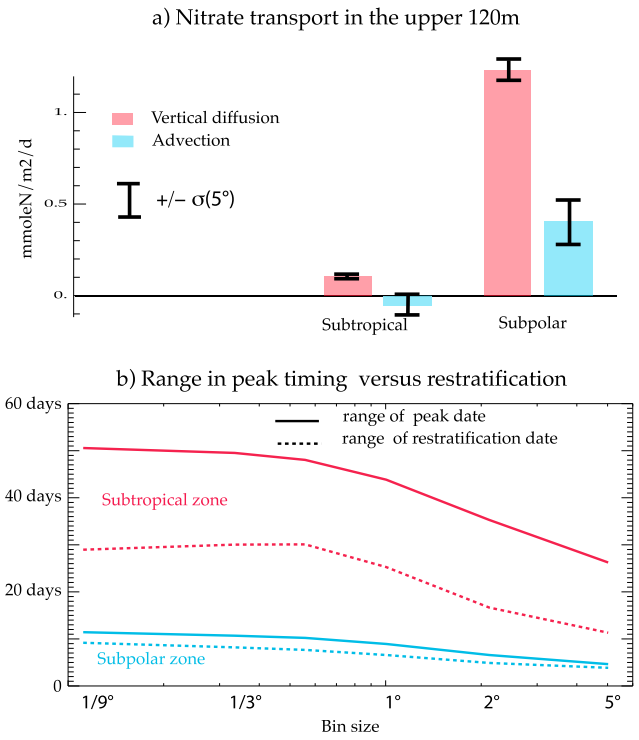

Figure 4. (a) Mean (color bars) $\pm\sigma$ (black horizontal lines) of the annual advective (blue) and diffusive (red) sources of nitrate into the upper 120 m, binned at 5° and averaged over the subtropical and subpolar zones shown in Figure 1a. (b) Range in bloom peak timing (reported from Figure 3b) against bin size, compared with the range in the restratification date (dashed line, defined as the date at which the mixed layer depth has shoaled above 50 m).

Due to computational and storage constraints, only 5 years of model outputs were available. Given this rather small number, we checked the accuracy of our estimate over the ocean color data set, for which 15 years were available. This was done by randomly selecting 5 of the 15 years, 100 times, and by computing the 25%–75% quartile over the 100 different estimates of σ (vertical lines in Figures 3a and 3b). This revealed a median accuracy of the order of 10% on peak amplitude and 5 days in peak timing. Our detected changes are well above this threshold error confirming the robustness of the results discussed in this paper.

Our model also revealed significant interannual variability in 5° binned annual new production, particularly in the subtropical gyre, of the order $\sim$20% (Figure 3c). The full strength of this signal could only be captured at fine ($\Delta x < 1/27°$) horizontal resolution (Figure 3d). This suggested that intermittent vertical advection at submesoscale fronts (whose full strength requires high resolution) could be responsible for the observed interannual variability. This was further confirmed by a more detailed analysis of the nitrate budget in the euphotic layer. This budget exhibited large interannual variability in the advective (and to a lesser extent, in the diffusive) supply of nitrate in both regions (Figure 4a). In the subtropics, the magnitude of this variability was large enough to overcome the mean advective loss of nitrate which resulted from downward Ekman pumping [*Lévy et al.*, 2012b]; hence, the actual sign of the annual nitrate supply to the subtropical zone varied interannually. The intermittent nature of these nitrate pulses also explained the variability in phytoplankton peak timing in the otherwise depleted subtropics with some of the peaks being in fact associated with such events (Figure 2a).

Another potential internal mechanism that could drive interannual variability in bloom peak timing is restratification by submesoscales [*Boccaletti et al.*, 2007]. This process induced interannual variations of the time at which the mixed layer shoaled between winter and spring in our model (dashed lines in Figure 4b). To test this hypothesis, we compared this restratification date range to the peak date range (Figure 4b). In the subtropics, the restratification date range was only about half of the peak date range illustrating that varying restratification times was not sufficient to explain the large variability in peak dates. Indeed, as mentioned before, part of this variability can be attributable to the time variability in nutrient supply pulses. However, in the subpolar zone, the two ranges are closer which supports the hypothesis that submesoscale stratification could be responsible for the simulated interannual variability in bloom timing. This is also illustrated in Figures 2b and 2d where a strong submesoscale front causes an earlier mixed layer shoaling and a phytoplankton peak occurring 1 week earlier in year 1 than in year 2. It should be reminded, however, that the effect of submesoscale restratification on bloom timing is rather small compared with the atmospherically driven variability (Figure 3a) and has only marginal consequences on the annual new production budget (Figure 3c).

5. Conclusion

A highly idealized model which showed features reminiscent of the North Atlantic phytoplankton bloom and eddy variability was used to investigate how internal variability associated with submesoscale fronts drove interannual variability in the bloom. The processes that have been highlighted are not specific to the North Atlantic and should also apply to the North Pacific or to the Southern Ocean. The advantage of using an idealized model was that it could be run at very high horizontal resolution. Our results suggested that transient nutrient supply by submesoscale fronts induced interannual variability in annual mean new production, hence, in export production [*Resplandy et al.*, 2012], over the scale of oceanic provinces. Another source of variability was restratification at these fronts which induced moderate variability in bloom timing. Such variability could only be captured with a model at submesoscale permitting resolution and rapidly decreased at coarser resolution. Comparison with variability in 5° binned ocean color data suggested that this internally driven variability is not small relative to climate-driven variability, which might explain the generally moderate levels of correlation between ocean color data and climate indices. At small scale, we found that internal variability could be as large as external variability, which calls for even more caution when trying to relate the variability observed from moorings or time series stations to climate indices.

The present results need to be confirmed in the frame of longer, more realistic, basin scale simulations, with variable interannual atmospheric forcings, which will also allow more rigorous comparison with the variability observed in the ocean and more robust statistics. However, they suggest that submesoscale permitting resolution is needed to capture the full strength of the variability. This is unlike internal variability of core physical properties, such as sea level anomaly, which could be captured at 1/4° resolution [*Penduff et al.*, 2011]. It relates to the paramount sensitivity of biogeochemistry to vertical fluxes which are much stronger at the submesoscale than at the mesoscale [*Capet et al.*, 2008].

Acknowledgments

This work was supported by Agence Nationale de la Recherche under the reference ANR-09-Blan-0365-03 REDHOTS. The simulations were performed at IDRIS (France) by C. Ethe from initial states computed on the Earth Simulator (ESC, Yokohama, Japan). We thank Thierry Penduff and Laurent Bopp for insightful discussions and two anonymous reviewers for their useful comments. The merged altimeter products were produced by Ssalto/Duacs and distributed by Aviso with support from CNES. The merged ocean color products were produced by the ESA GlobColour project.

The Editor thanks Pete Gaube and an anonymous reviewer for their assistance in evaluating this paper.

References

Behrenfeld, M. (2010), Abandoning Sverdrup's Critical Depth Hypothesis on phytoplankton blooms, *Ecology*, *91*(4), 977–989.

Behrenfeld, M., R. O'Malley, D. Siegel, C. McClain, J. Sarmiento, G. Feldman, A. Milligan, P. Falkowski, R. Letelier, and E. Boss (2006), Climate-driven trends in contemporary ocean productivity, *Nature*, *444*(7120), 752–755.

Boccaletti, G., R. Ferrari, and B. Fox-Kemper (2007), Mixed layer instabilities and restratification, *J. Phys. Oceanogr.*, *37*, 2228–2250.

Capet, X., J. McWilliams, M. Molemaker, and A. Shchepetkin (2008), Mesoscale to submesoscale transition in the California Current System. Part I: Flow structure, eddy flux, and observational tests, *J. Phys. Oceanogr.*, *38*, 29–43.

Chavez, F. P., M. Messié, and J. T. Pennington (2011), Marine primary production in relation to climate variability and change, *Annu. Rev. Mar. Sci.*, *3*(1), 227–260.

Cole, H., S. Henson, A. Martin, and A. Yool (2012), Mind the gap: The impact of missing data on the calculation of phytoplankton phenology metrics, *J. Geophys. Res.*, *117*, C08030, doi:10.1029/2012JC008249.

Cole, H. S. (2013), The natural variability and climate change response in phytoplankton phenology, PhD thesis, 340 pp., Univ. of Southampton, Southampton, U. K.

Follows, M., and S. Dutkiewicz (2001), Meteorological modulation of the North Atlantic spring bloom, *Deep Sea Res., Part II*, *49*(1), 321–344.

Hazeleger, W., and S. Drijfhout (2000), A model study on internally generated variability in subtropical mode water formation, *J. Geophys. Res.*, *105*, 13,965–13,979.

Henson, S. A., I. Robinson, J. T. Allen, and J. J. Waniek (2006), Effect of meteorological conditions on interannual variability in timing and magnitude of the spring bloom in the Irminger Basin, North Atlantic, *Deep Sea Res., Part I*, *53*(10), 1601–1615.

Huck, T., G. K. Vallis, and A. Colin de Verdiere (2001), On the robustness of the interdecadal modes of the thermohaline circulation, *J. Clim.*, *14*, 940–963.

Karleskind, P., M. Lévy, and L. Memery (2011), Modifications of mode water properties by sub-mesoscales in a bio-physical model of the Northeast Atlantic, *Ocean Modell.*, *39*, 47–60.

Levy, M., L. Memery, and G. Madec (1998), The onset of a bloom after deep winter convection in the northwestern Mediterranean sea: Mesoscale process study with a primitive equation model, *J. Mar. Syst.*, *16*(1-2), 7–21.

Lévy, M., P. Klein, and A. Treguier (2001), Impact of sub-mesoscale physics on production and subduction of phytoplankton in an oligotrophic regime, *J. Mar. Res.*, *59*(4), 535–565.

Lévy, M., P. Klein, A. M. Tréguier, D. Iovino, G. Madec, S. Masson, and K. Takahashi (2010), Modifications of gyre circulation by sub-mesoscale physics, *Ocean Modell.*, *34*(1-2), 1–15.

Lévy, M., R. Ferrari, P. J. S. Franks, A. P. Martin, and P. Rivière (2012a), Bringing physics to life at the submesoscale, *Geophys. Res. Lett.*, *39*, L14602, doi:10.1029/2012GL052756.

Lévy, M., D. Iovino, L. Resplandy, P. Klein, G. Madec, A. M. Tréguier, S. Masson, and K. Takahashi (2012b), Large-scale impacts of submesoscale dynamics on phytoplankton: Local and remote effects, *Ocean Modell.*, *43-44*(C), 77–93.

Lévy, M., L. Resplandy, P. Klein, X. Capet, D. Iovino, and C. Ethé (2012c), Grid degradation of submesoscale resolving ocean models: Benefits for offline passive tracer transport, *Ocean Modell.*, *48*(C), 1–9.

Madec, G. (2008), NEMO ocean engine, *Note du Pole de modelisation de l'Institut Pierre-Simon Laplace*, *27*, 1–217.

Martinez, E., D. Antoine, F. D'Ortenzio, and B. Gentili (2009), Climate-driven basin-scale decadal oscillations of oceanic phytoplankton, *Science*, *326*(5957), 1253–1256.

Mahadevan, A, E. D'Asaro, C. Lee, and M. Perry (2012), Eddy-driven stratification initiates north atlantic spring phytoplankton blooms, *Science*, *337*(6090), 54–58.

McGillicuddy, D., A. Robinson, D. Siegel, H. Jannasch, R. Johnson, T. Dickey, J. McNeil, A. Michaels, and A. Knap (1998), Influence of mesoscale eddies on new production in the Sargasso Sea, *Nature*, *394*(6690), 263–266.

Penduff, T., B. Barnier, W. K. Dewar, and J. J. O'Brien (2004), Dynamical response of the oceanic eddy field to the North Atlantic Oscillation: A model-data comparison, *J. Phys. Oceanogr.*, *34*(12), 2615–2629.

Penduff, T., M. Juza, B. Barnier, J. Zika, W. K. Dewar, A.-M. Treguier, J.-M. Molines, and N. Audiffren (2011), Sea Level expression of intrinsic and forced ocean variabilities at interannual time scales, *J. Clim.*, *24*(21), 5652–5670.

Poggiale, J. C., Y. Eynaud, and M. Baklouti (2013), Impact of periodic nutrient input rate on trophic chain properties, *Ecol. Complexity*, *14*, 56–63.

Resplandy, L., A. P. Martin, F. Le Moigne, P. Martin, A. Aquilina, L. Mémery, M. Lévy, and R. Sanders (2012), How does dynamical spatial variability impact 234Th-derived estimates of organic export?, *Deep Sea Res., Part I*, *68*(C), 24–45.

Rousseaux, C., and W. Gregg (2014), Interannual variation in phytoplankton primary production at a global scale, *Remote Sens.*, *6*(1), 1–19.

Thomas, M. D., and X. Zhai (2013), Eddy-induced variability of the meridional overturning circulation in a model of the North Atlantic, *Geophys. Res. Lett.*, *40*, 2742–2747, doi:10.1002/grl.50532.

Williams, R. G., C. Wilson, and C. W. Hughes (2007), Ocean and atmosphere storm tracks: The role of eddy vorticity forcing, *J. Phys. Oceanogr.*, *37*(9), 2267–2289.